

# Assessment of dose rate profiles and accessibility inside the building of the experimental fusion reactor, ITER, during operation and after shutdown

Mahmoud Youssef <sup>a,\*</sup>, Anil Kumar <sup>a</sup>, Mohamed Abdou <sup>a</sup>, Hesham Khater <sup>b</sup>,  
Mohamed Sawan <sup>b</sup>, Douglas Henderson <sup>b</sup>

<sup>a</sup> *Mechanical and Aerospace Engineering Department, University of California, Los Angeles, CA 90095, USA*

<sup>b</sup> *Fusion Technology Institute, University of Wisconsin, Madison, WI 53706-1687, USA*

## Abstract

During the D–T operation of the International Thermonuclear Experimental Reactor (ITER), the dose inside ITER building is attributed to neutrons and gamma-rays streaming from various openings in the machine, whereas after shutdown, it is solely due to the decay gammas from activated components inside the building. In the present study, two cases of different geometrical arrangement are considered (Case A and Case C) in which the impact of the size of the opening of the NBI horizontal ports and presence of the NBI structure on the dose profiles everywhere in ITER building was studied and compared to the case (Case B) where all the horizontal ports are plugged. Contours and mapping of the dose rate profiles during operation, at shutdown, and at one-day, one-week, and one-month after shutdown, were generated for the three cases. Zone classification requirements for each hall/room and gallery of the building in terms of the maximum allowed exposure dose during operation and after shutdown were examined to identify where these requirements are met during ‘hands-on’ maintenance activities. It is shown that the requirements are satisfied at all times after shutdown in the halls above the ground, even during operation. For the conservative Case A, the dose rates are excessively high inside the equatorial NBI hall and inside the access halls above and below (divertor hall). In Case C, all the halls/vaults and galleries are accessible 1-week after shutdown, except inside the NBI hall whose dose rate ( $6.2 \times 10^5 \mu\text{Sv h}^{-1}$ ) exceeds the required zone classification ( $3\text{--}10 \mu\text{Sv h}^{-1}$ ). All areas are accessible a week after shutdown in Case B which represents the building side away from the NBI ports. However, in all these cases, the accessibility criterion inside the rooms beneath the cryostat is not met at all times after shutdown due to the rather thin bottom bioshield (50 cm) which may necessitate some design changes. © 1998 Elsevier Science S.A. All rights reserved.

## 1. Introduction:

During the D–T operation of the International Thermonuclear Experimental Reactor (ITER),

neutrons and gamma-rays will stream through the various large openings surrounding the machine. Accurate assessment of exposure dose inside ITER building during both operation and after shutdown is required to: (a) identify the hot locations where human accessibility is prohibited; and

\* Corresponding author. Tel.: +1 310 8252879.

(b) evaluate the required waiting period after shutdown and locations where this accessibility is allowed for maintenance purposes. The dose during operation is attributed to leaked neutron and gamma radiation whereas after shutdown, it is solely due to decay gammas from activated components inside the building, including the concrete walls. The exposure dose distribution is highly dependent on the operation scenarios under which this assessment is made. For example, when the machine is open through the vertical port and the plasma region is exposed or divertor cassettes are being transported, this dose distribution will differ from the case where the machine is shutdown when only the horizontal ports (including the NBI ports) are open during operation. The present work focuses on this latter operation scenario. More details of present work can be found in Youssef et al. [1].

The large vacuum chamber, the cryostat, is a right circular cylinder, surrounding the massive Tokamak machine, with a diameter of  $\sim 36$  m. The embedded portion of ITER building, which surrounds the cryostat, is described as the Tokamak pit. It is also a right circular cylinder placed under ground. The pit is made of a triple cylinders, the inner most of which is the biological shield that has radial openings which allow components transport through the pit halls (4) and vaults (2) to the outer pit galleries (3). Two rectangular buildings (the tritium and the power termination buildings) are structurally attached to the pit with a part embedded under ground. The Assembly Hall, the Laydown Hall and the Tokamak Hall are structural buildings that mainly stand above ground and house the overhead bridge cranes. Fig. 1 is the east–west view of ITER building where the various halls/vaults and galleries are shown [2,3].

The dose assessment in the present work is made under the operation scenario that the vertical port and the divertor port are plugged during operation. As for the horizontal ports, three distinct cases were analyzed in which the horizontal ports are open in two cases and totally plugged in the third case. Additionally, no equipment were assumed to be present inside the building (except in one case where the NBI structure is present)

whose activation during the reactor operation is not considered in the present analysis. Likewise, activation inside the cooling pipes and other parts of the heat removal system that extend inside the building was also not accounted for. The analysis is focused on the underground part of ITER building, however, a limited part of the upper ground buildings is considered in the model. Dose rate profiles during operation and at various times after shutdown were generated everywhere in the building. Zone classification requirements for each access area in terms of the maximum allowed exposure dose were examined to identify where these requirements are met during ‘hands-on’ maintenance activities.

## **2. Computational approach models and cases analyzed**

Due to the large size of Tokamak, including its internals (ports, FW, blanket, backplates, etc.) and the large size of the ITER building itself (50 m underground depth, 54 m radius), including the rectangular attached buildings, it was necessary to break down the problem into several models where neutrons and gamma rays transport is carried out in one model to generate the required external source needed as input to the second model, and so on. Since dose rate mapping in ITER building is the prime objective of the analysis, all of these calculations were carried out using deterministic methods, namely, by utilizing the 2-D and 3-D discrete ordinates codes, DORT TORT [4]. This calculational approach has the advantage of determining the nuclear field at each spatial location but on the expense of requiring several gigabytes of the computer disk space to hold fluxes files and other auxiliary files. The Monte Carlo method was used, however, to calculate dose rate at specific locations, as outlined in a separate paper [5].

### *2.1. Approach and calculational models*

The calculational procedures followed are as follows:

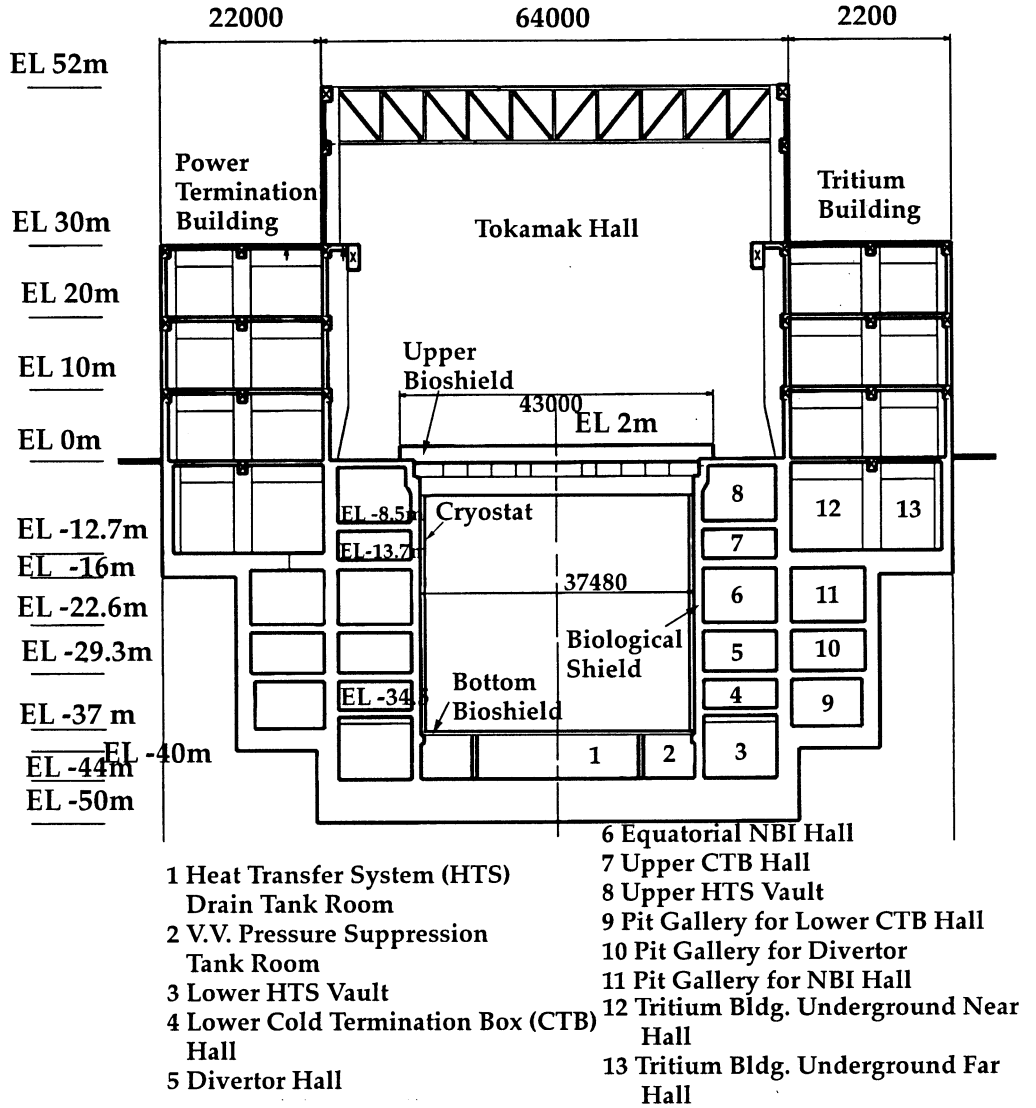


Fig. 1. East-west cross section view of ITER Tokamak building.

(1) Firstly, the internal boundary source (IBS) at the outer surface of the cryostat was calculated and obtained from 2-D  $R-Z$  DORT model of the Tokamak internals, considering all of the geometrical and material arrangement inside the cryostat. Fig. 2(a) shows the 2-D Tokamak model of Case C. A fixed discrete spatial mesh ( $258 \times 307$   $R-Z = 79206$  mesh) was utilized based on previous analysis of ITER Tokamak (S. Sato, Japan Atomic Energy Research Institute (JAERI), 1996,

private communication). However, it was necessary in this previous model to modify the spatial boundaries such that the  $R$  and  $Z$  boundaries of Tokamak model (Fig. 2a) and the ITER building model (Fig. 2b) are common in the two 2-D  $R-Z$  models. The Tokamak model was solved using the FUSION40 library [6] (42n-21g) based on JENDL-3.1 with P5S6 approximation. The generated initial IBS at the cryostat boundaries was further treated and resolved by: (a) converting

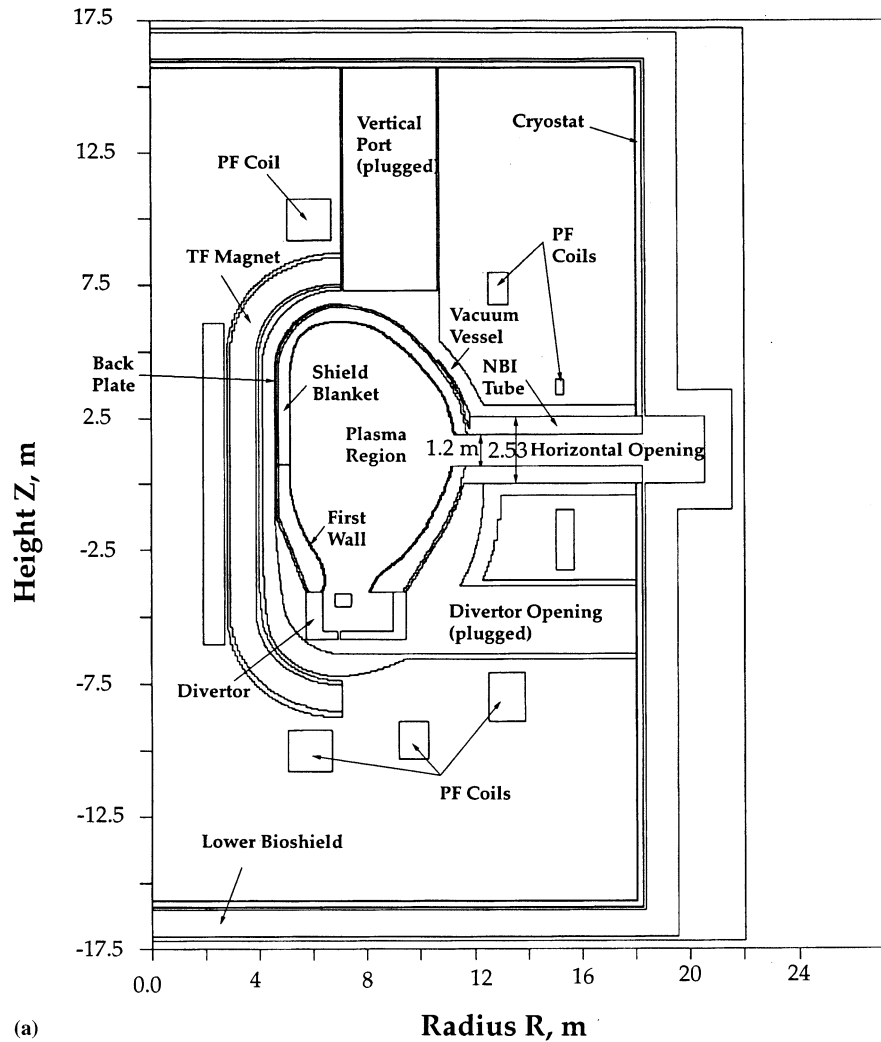


Fig. 2. Two-dimensional  $R$ - $Z$  calculational models of Case C: (a) Tokamak model, (b) Building model.

neutron and gamma angular fluxes to  $46n$ - $21g$  group structure used in the building model; (b) collapsing these fluxes from fine mesh boundaries to broad mesh boundaries used in the building model; and (c) adding finer spatial meshes, where necessary, at locations where meshes in the Tokamak model were judged to be too broad to be utilized in the DORT 2-D model of the building;

(2) The BNDRY code of the DORT/TORT package was used to reformulate the final IBS in the format required as an IBS to the subsequent 2-D DORT run for the building model (Fig. 2b) in which the cryostat, the pit, the pit

galleries and the under ground part of the Tritium and Power Termination buildings were modeled in 2-D  $R$ - $Z$  geometry. Part of the Tokamak Hall, and Tritium and Power Termination buildings above the ground level are considered in the model. With the exception of these rectangular buildings, the other parts of an ITER building are cylindrical in shape. It is more accurate, therefore, to consider  $R$ - $Z$ - $\theta$  or  $R$ - $Z$  modeling. The dirt surrounding the underground part of the building was accounted for in the model. To maintain higher accuracy, small mesh size was considered in order to assess flux attenuation in  $R$  and  $Z$

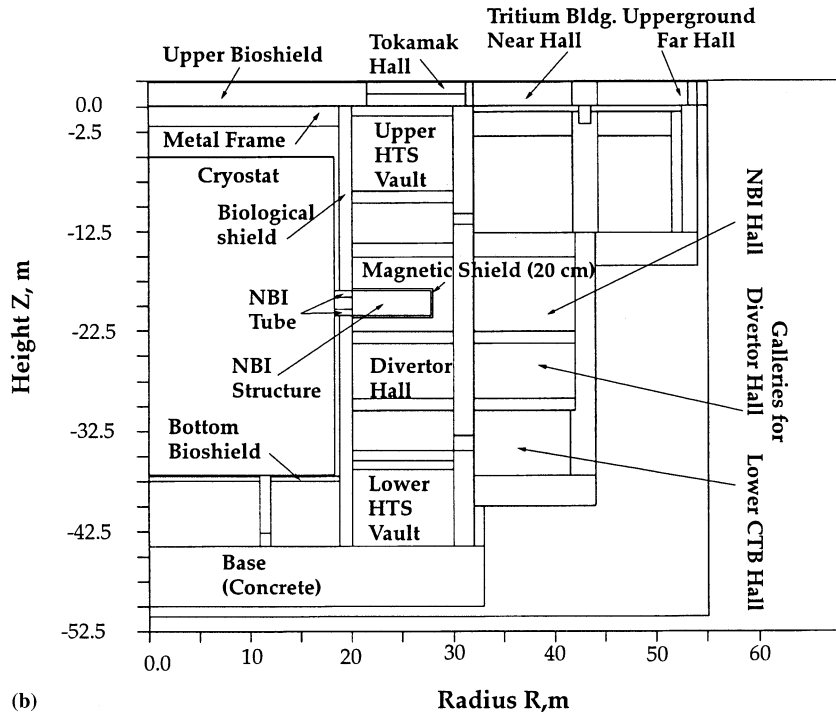


Fig. 2. (Continued)

directions where large geometrical variations are encountered. The geometrical variation in the  $\theta$  direction is minimal and therefore, the building was modeled in  $R$ - $Z$  geometry. The T. and P.T. buildings were approximated as cylinders. Accurate assessment of dose rates in these buildings were obtained from subsequent 3-D runs. In the building 2-D  $R$ - $Z$  model, the NBI opening is considered continuous in the azimuthal direction (Cases A and C, see below). The openings in the pit wall at the halls of the upper and lower cold termination box (CTB, and named upper and lower feed magnet area in Fig. 1) are assumed open. Since an IBS was used in the model, the zone inside the cryostat was treated as one material consisted of 70% SS316-30% Water diluted by a factor of 0.07. Therefore, the results given here inside the cryostat has no practical meaning. It was shown, that the results outside the cryostat are insensitive to the dilution factor. The calculations were performed with P5S6 approximation using 46n-21g cross-section library generated from the FENDL/MG-1.0 [7,8] multi-group database

(MATXS format) using the TRANSX-2 processing code [9]. Nine discontinuous mesh description sets were utilized to describe the spatial boundaries of the building model. This was necessary to avoid using fine mesh description inside the air of the various halls/rooms and galleries if a fixed spatial set were to be used instead which could make the number of meshes applied prohibitively large. Utilizing these nine sets resulted in using a relatively lower number of meshes (116921 mesh).

(3) The angular flux file around the Tritium (and the identical power termination) building is generated from the previous step along with the flux moment file to the entire model. These files are inputted to the VISA code of the DORT/TORT package [4] to correct for the last iteration in the previous DORT run and generate the required input file for the TORSSED code [4]. This later code generates a 3-D external boundary source from the previous 2-D  $R$ - $Z$  run for the subsequent  $X$ - $Y$ - $Z$  run of TORT code. Half of the Tritium building (38 m long in the  $Y$  direc-

tion, going into paper) was modeled using  $129 \times 30 \times 89$  ( $= 344430$ ) mesh description. The dose rate mapping inside the T. and the P.T. buildings were re-assessed from the 3-D calculations and compared to the 2-D results.

(4) The neutron and gamma fluxes during operation are then used to calculate the operational dose at each spatial location using the flux-to-dose conversion factors of ICRP [10]. These fluxes are also used as input to DKR-PULSAR-1.0, the latest updated version of DKR-ICF code [11] to generate the decay gamma source intensity at shutdown, 1-day, 1-week, and 1-month after shutdown. A separate gamma transport run (DORT/TORT run for the  $R-Z/X-Y-Z$  model, respectively) is then performed for each time after shutdown to calculate the transported gamma fluxes everywhere in the building and the corresponding dose rates.

## 2.2. Cases analyzed

The cases considered in the present work are as follows:

### 2.2.1. Case A

This is the reference and most conservative case in which the aperture of the horizontal NBI opening at the blanket first wall is  $\sim 2.53$  m in height and the FW/blanket/backplate are removed (as shown in Fig. 2(a) with the NBI tube removed and Fig. 2(b) with the NBI structure removed). In the two 2-D models, this opening is considered continuous in the azimuthal direction and this tends to over estimate the dose rate everywhere in the building, particularly inside the NBI hall. In reality, there are twenty of such horizontal openings. If dose rate distribution inside ITER building was acceptable under this very conservative assumption, it would also be acceptable under any other more realistic assumption in modeling the NBI port. It was found, however, that the dose rates are excessively high inside some rooms (e.g. the NBI hall, the Divertor hall, etc.) which motivated the analyses of Case B and Case C.

### 2.2.2. Case B

In this Case (see Fig. 3), the FW/blanket/backplate are placed in front of the horizontal openings and the bioshield opening in ITER building is closed (as in Fig. 2(b) with the NBI structure and tube removed). This geometrical configuration corresponds to a closed opening away from the NBI ports and thus gives estimates to the lowest dose rate distribution in ITER building, subject to the assumption that neutrons and gamma-rays streaming out of the open NBI ports on the other side will not contribute at all.

### 2.2.3. Case C

Fig. 2(a, b) show the Tokamak and ITER building calculational models of Case C, respectively. The opening in the FW, blanket, and backplate correspond to the 1.2 m aperture of the NBI tube which is also included in the model as shown in Fig. 2(a). This tube (duct) is also extended inside the bioshield and leads to the NBI structure and magnetic shield. This case is a more realistic representation of the NBI port since it accounts for the attenuation of the radiation field resulting from the presence of the NBI structure which considered to be composed of the inner homogenized structure (assumed to be 5% density of 90% SS316 + 10% Cu mixture) and the outer magnetic shield layer (20 cm thick and made of 100% SS316). The length of NBI considered in this analysis is 8 m.

## 3. Zone classification and access to ITER rooms and galleries

According to the accessibility criteria adopted for ITER [12], there will be no requirement for personnel access to areas of ITER plant which are inside the Tokamak Hall and below ground level during operation. This part of the building is classified as Zone D (Table 1). When the plasmas are not burning and during maintenance operations, hands-on maintenance activities will be performed. During this time, other zone classifications have been identified [12] as the desired zone designation as Zone A, B1, B2, or C (Table 1). In Fig. 1, the required zone classifica-

Table 1  
ITER personnel radiation zones [13]

Zone	Name	Dose rate ( $\mu\text{Sv h}^{-1}$ )	Type of entry permitted
Zone A	Free area	<0.5	Without dosimetry and radiological control
Zone B1	Supervised area	0.5–3	Dosimetry, unlimited entry within working hours
Zone B2	Controlled area	3–10	Dosimetry, unlimited entry within working hours, well established procedures and practices to control radiation exposure
Zone C	Time limited entry area	10–100	Dosimetry, time limited entry, well established procedures and practices to control radiation exposure
Zone D	Restricted entry area	> 100	Dosimetry, entry permitted for brief periods of time under special circumstances

tion in each room/hall/vault for hands-on maintenance after shutdown are as follows: Room 1 (B2), Room 2 (B2), Vault 3 (C), Hall 4 (B2), Hall 5 (B2), Hall 6 (B2), Hall 7 (B2), Vault 8 (C), Gallery 9 (B2), Gallery 10 (B2), Gallery 11 (B2), Hall 12 (B2), and Hall 13 (B2). The latter two halls in the underground part of the power termination building is designated as zone B 1 instead as shown in Fig. 4. All of the halls/rooms above the ground are designated as zone B1. We examined whether or not these criteria are met during operation and during ‘hands-on’ maintenance activities after shutdown.

## 4. Results and discussion

### 4.1. Case A

#### 4.1.1. Flux profile in the radial direction

In Case A, the neutrons flux during operation is in the order of  $1.0 \times 10^{13}$   $\text{n}(\text{cm}^2 \text{s})$  at the mouth of the NBI opening. Neutron flux attenuation through the bioshield (1.26 m-thick) is dependent upon the  $Z$  level. The flux attenuates by 5–6 orders of magnitude at this radial location. Likewise, flux attenuation through the outer pit wall is also dependent upon the  $Z$  level (5–7 orders of magnitude). Fig. 5 shows the radial attenuation of the total neutron flux at  $Z = -13.7$  m (floor of the upper CTB hall),  $Z = -20$  m (middle of NBI opening) and  $Z = -22.60$  (floor of the NBI Hall). Neutron flux

through the NBI penetration itself is attenuated by a factor of  $\sim 2$  and by an order of magnitude throughout the NBI Hall (from  $R = 18.74$ – $30$  m). The largest attenuation through the outer pit wall is at  $-44$  m level (11 orders of magnitude, not shown).

#### 4.1.2. Flux profile in the axial direction

At the outer surface of the bioshield ( $R = 20$  m), neutron flux in the axial direction varies from  $\sim 1 \times 10^{13}$   $\text{n}(\text{cm}^2 \text{s})$  (at the NBI opening) down to  $\sim 1 \times 10^3$   $\text{n}(\text{cm}^2 \text{s})$ , as can be seen from Fig. 6. The corresponding flux at the outer surface of the inner pit wall ( $R = 32$  m) varies from  $1 \times 10^5$   $\text{n}(\text{cm}^2 \cdot \text{s})^{-1}$  down to  $\sim 1 \times 10^{-6}$   $\text{n}(\text{cm}^2 \cdot \text{s})^{-1}$ .

The attenuation characteristics of the slabs also vary in the axial direction. The slab above the NBI room (1.4 m-thick,  $Z = -13.7$  m) has an attenuation power of approximately an order of magnitude for every  $\sim 23$  cm. The slab below the NBI room (1.2 m-thick,  $Z = -29.3$  m) has an attenuation power of approximately an order of magnitude for every  $\sim 25$  cm.

#### 4.1.3. Dose rate profiles

Fig. 7 shows the maximum dose rate attainable inside each room and gallery during operation and at various time after shutdown. The maximum dose rate during operation is inside the equatorial NBI hall ( $1.0 \times 10^{13}$   $\mu\text{Sv h}^{-1}$ ) and the least maximum dose rate is inside the Tritium building upper ground far hall ( $\sim 4.6 \times 10^4$   $\mu\text{Sv h}^{-1}$ ). Large dose values are found in

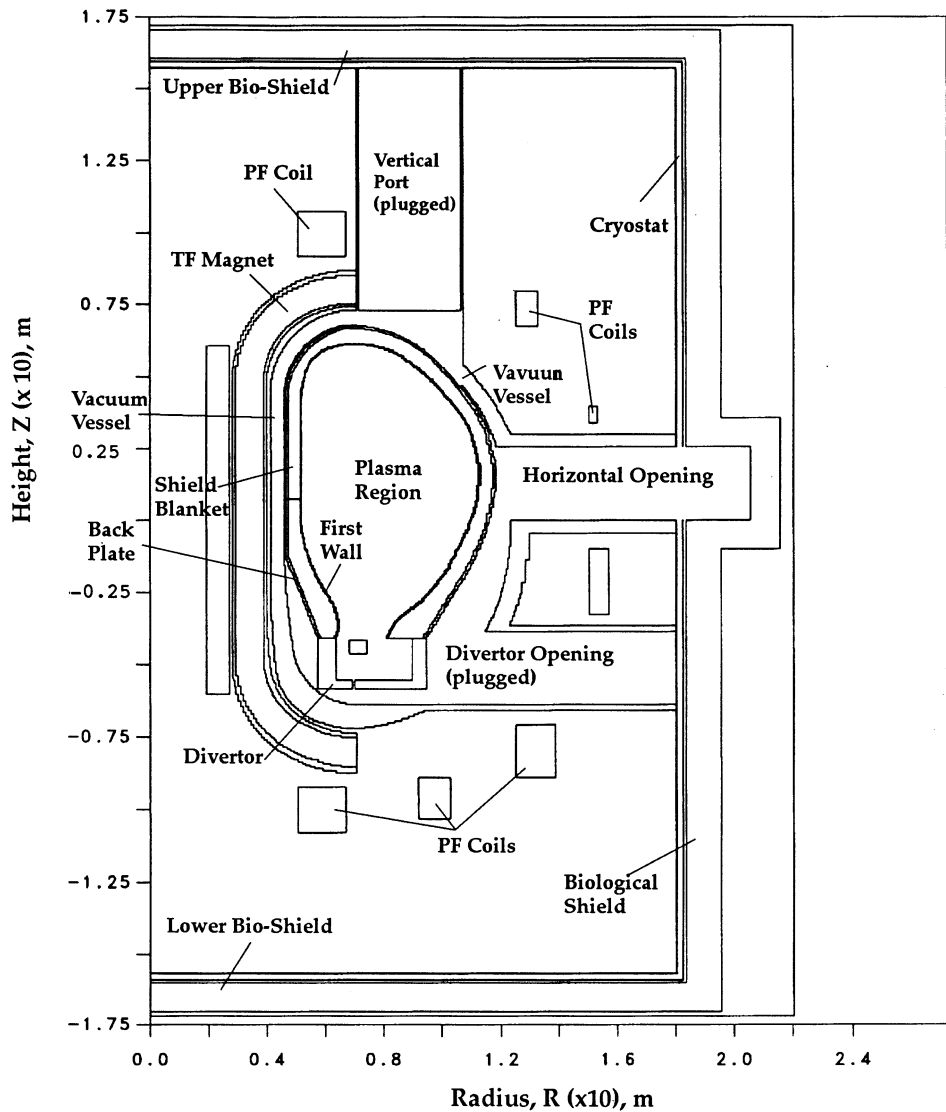


Fig. 3. Two-dimensional  $R$ - $Z$  calculational models of Case B: Tokamak model.

the halls close to the NBI hall and inside the rooms underneath the cryostat, whereas lower values are estimated inside the lower two pit galleries. Contours of dose rates during operation are shown in Fig. 8 (note that markers repeat after rate  $1.0 \times 10^{-5} \mu\text{Sv h}^{-1}$ ). The ratio of maximum to minimum dose varies among halls, galleries and rooms. This ratio is  $\sim 30$  inside the Equatorial NBI hall and  $\sim 1000$  inside the Pit gallery for Lower CTB hall.

The isosurfaces of a given dose rate inside the underground part of the Tritium building during operation were calculated from the 3-D  $X$ - $Y$ - $Z$  model and are shown in Fig. 9 for half of the building. The largest dose rate inside the Near Hall is  $\sim 1000 \mu\text{Sv h}^{-1}$  which is consistent with the contour for that value shown in Fig. 8 and obtained from the 2-D model. The low value of  $10 \mu\text{Sv h}^{-1}$  inside the far Hall is also consistent with the 2-D results which confirm approximating

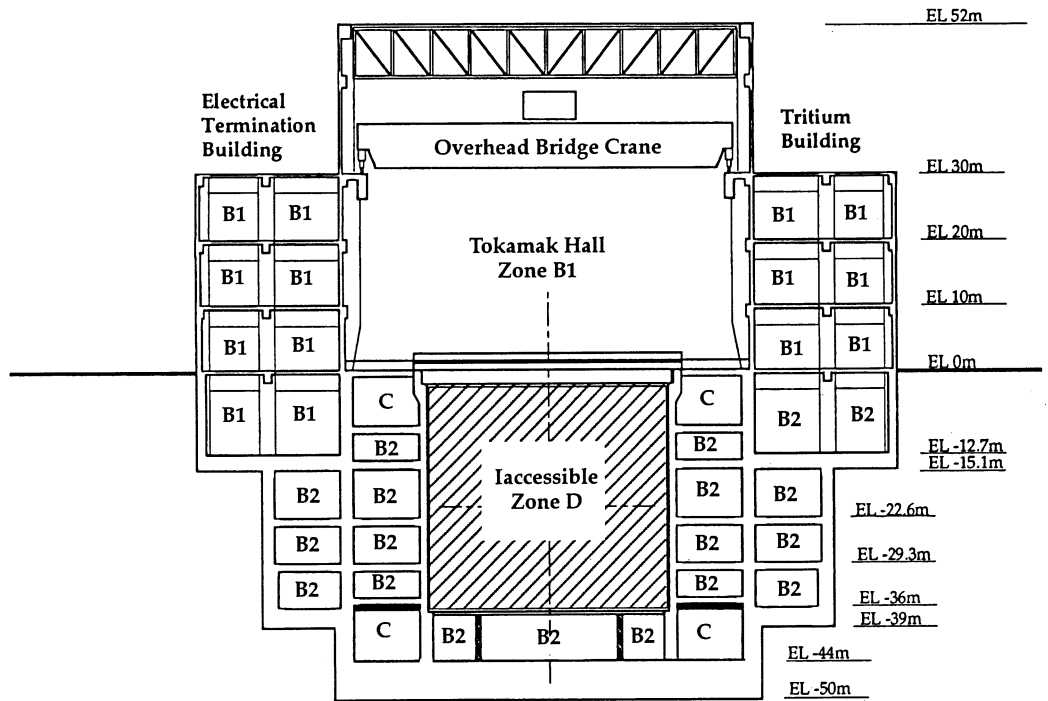


Fig. 4. Zone classification for accessibility inside ITER building for ‘Hands-on maintenance activities after shutdown’.

the rectangular part of the building as cylindrical geometry is a satisfactorily approximation, at least to the lower part of that building, and no further 3-D transport and activation analyses were pursued to that building. Note that lower rate values ( $0.1$  and  $1 \mu\text{Sv h}^{-1}$ ) occur inside the concrete wall, which is not of interest to the present study.

#### 4.1.4. Accessibility to the building

According to the accessibility criteria cited in Section 3, all zones above the ground are accessible, even during operation. Additionally, the dose rates inside the underground part of the Tritium building are low and meet zone classification requirements one week after shutdown (Fig. 7 and

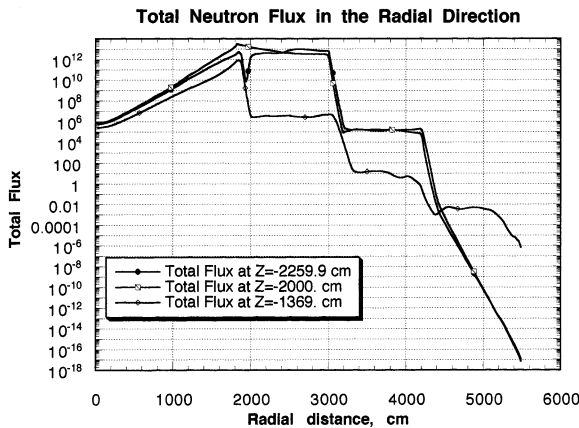


Fig. 5. Radial attenuation of total neutron flux during operation, Case A.

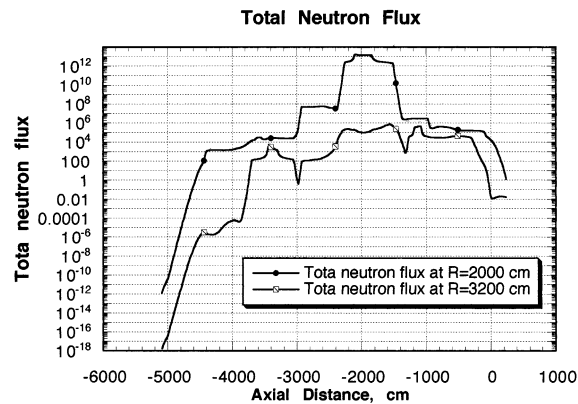


Fig. 6. Axial attenuation of total neutron flux during operation, Case A.

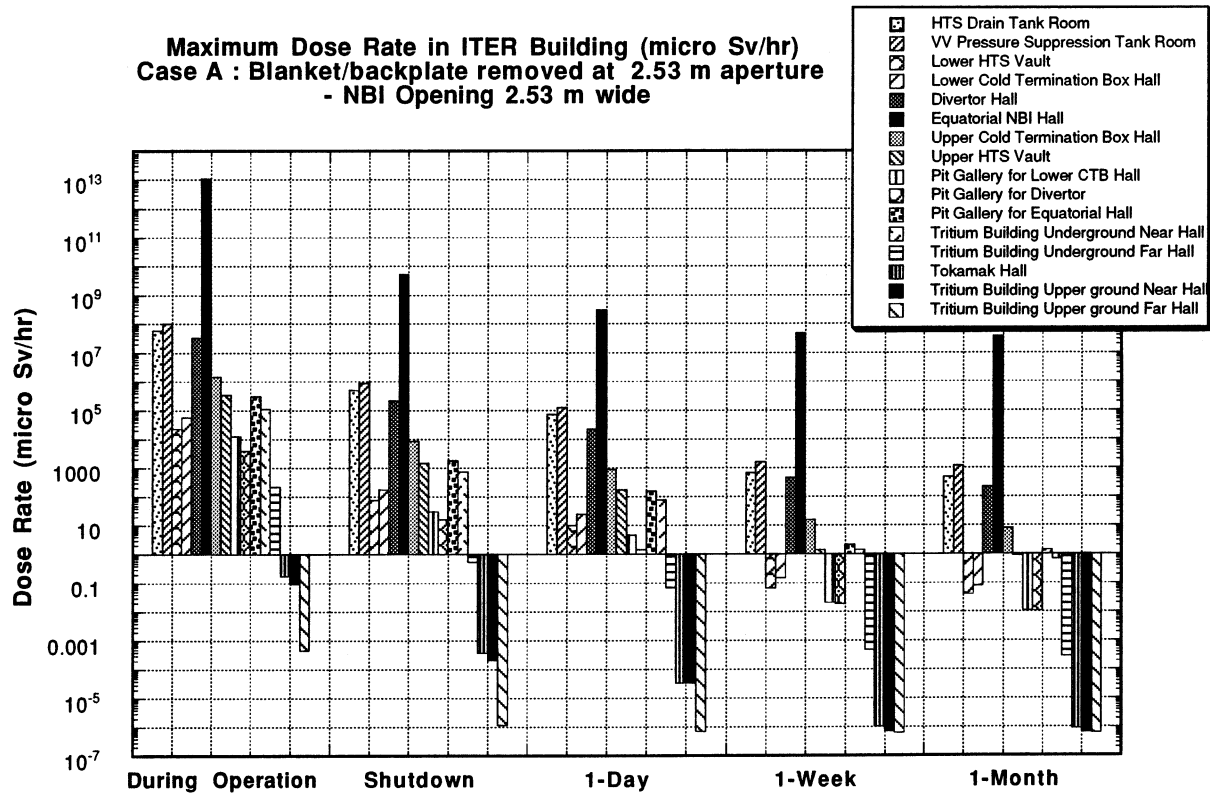


Fig. 7. Maximum dose rate inside each hall/room and gallery of ITER building during operation and at various times after shutdown, Case A.

Table 1). The highest dose rate a week after shutdown is in the NBI Hall ( $\sim 5 \times 10^7 \mu\text{Sv h}^{-1}$ ), the V.V. pressure suppression tank room ( $1.6 \times 10^3 \mu\text{Sv h}^{-1}$ ), and the Divertor hall ( $470 \mu\text{Sv h}^{-1}$ ), in that order. These are excessive dose rates that do not meet the zone classification requirement of B2 ( $3\text{--}10 \mu\text{Sv h}^{-1}$ ) even after one month from shutdown.

#### 4.2. Case B and Case C

Case B was considered to give credit to the fact that, with the exception of the three NBI openings, all the other 17 horizontal ports are closed during operation and hence, the dose rates in the halls/rooms and galleries that are on the opposite side of the NBI ports will be considerably less than the values found for Case A. Case C is similar to Case A, however, the open aperture at

the FW is much less (1.2 m height) and the NBI structure itself is included. Due to Case C being more representative of the actual geometrical arrangement, most of the discussion that follows focuses on this case.

Figs. 10 and 11 show the maximum dose rate in each access area in Case B and Case C. Fig. 10 shows the color (shaded) mapping of the dose rates at shutdown for Case C. Contours of iso-values are also shown. Color (shaded) mapping inside the NBI Hall and around the NBI structure of Case C is shown in Fig. 13. Numerical values can be inferred from the color (shaded) bars (e.g.  $-2$  means  $1.0 \times 10^{-2} \mu\text{Sv h}^{-1}$ ). From Figs. 10–13, the following can be stated:

(1) During operation, the maximum dose rate inside the equatorial NBI hall in Case C is  $\sim 5 \times 10^{10} \mu\text{Sv h}^{-1}$  and thus drops by a factor of  $\sim 218$  compared to Case A value of  $\sim 1 \times 10^{13} \mu\text{Sv h}^{-1}$ .

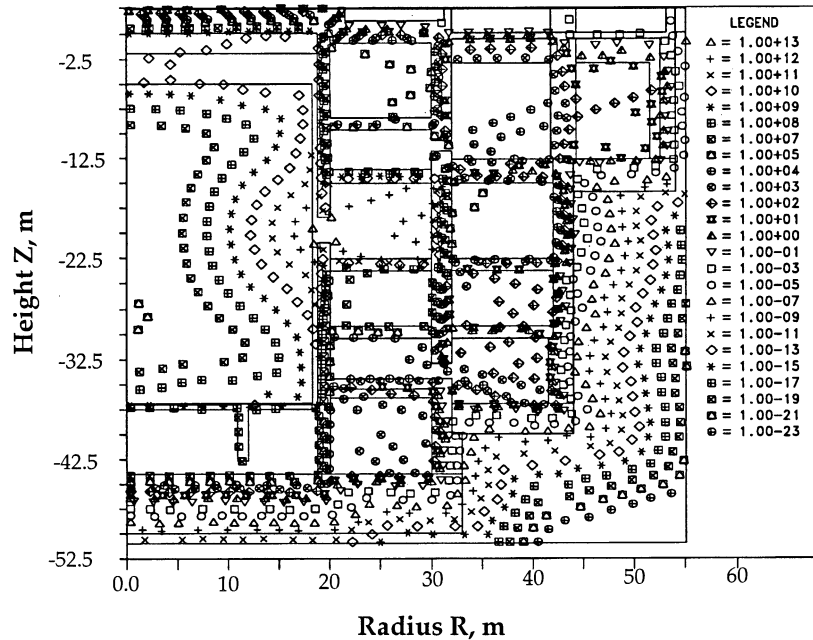


Fig. 8. Contours of dose rate profiles inside ITER building during operation, Case A.

This is the maximum value estimated in the open air area outside the NBI structure shown in Fig. 2(b). The dose rates inside the divertor hall and the upper CTB hall are reduced by a factor of  $\sim 219$  and  $\sim 58$ , respectively. In Case B, the dose rate in the NBI hall drops by almost 8 orders of magnitude due to the closure of the bioshield opening and the presence of the FW, blanket, and backplate. The closed bioshield (1.26-m thick) attenuates the incident nuclear field by roughly 5 orders of magnitude with the remaining reduction being attributed to the attenuation in the FW/blanket and backplate. The dose rates inside the divertor hall and the upper CTB access area are reduced by a factor of  $\sim 350$  and  $\sim 1185$ , respectively.

(2) During operation, the dose rates in the access area below the cryostat is as large as  $\sim 1.0 \times 10^7 \mu\text{Sv h}^{-1}$  in Cases B and C ( $\sim 1.0 \times 10^8 \mu\text{Sv h}^{-1}$  in Case A). The lower values for Case B and C compared to Case A are due to the change in the spectrum of neutrons and gamma rays reaching this access area. This change resulted from placing (or partially placing) the FW, blanket, and backplate in front

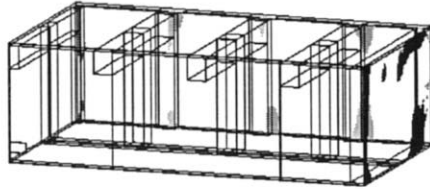
of the NBI opening.

(3) At shutdown, reduction of  $\sim 2$ – $3$  orders of magnitude in dose rates occurs. In the NBI Hall, a reduction in the maximum dose rate of more than  $\sim 3$  orders of magnitude takes place in Case A (reduction of  $\sim 2$  orders of magnitude in Case B and  $\sim 3$  orders of magnitude in Case C).

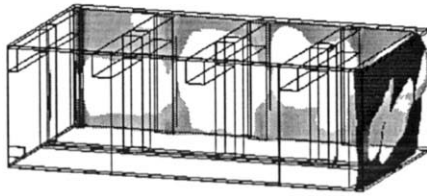
(4) An additional reduction of 1 order of magnitude in dose rates occurs at 1-day after shutdown, particularly for rooms closer to the cryostat. The dose rates in the halls above ground almost assume no further reduction from the shutdown values, except for Case A.

(5) Compared to dose rate distribution at 1-day after shutdown, the reduction in dose rates after 1 week from shutdown varies from one room to another. The reduction is a factor of  $\sim 200$ ,  $\sim 100$ , and  $\sim 100$  in the Pit Gallery for Lower CTB Hall in Case A, B, and C while it is a factor of  $\sim 7$ ,  $\sim 100$ , and  $\sim 7$  in the NBI Hall in Case A, B, and C, respectively. Note that the reduction in Case B is larger in this hall compared to Case A and C due to the rapid decay of radio nuclides generated mainly in the concrete rather than from the SS316.

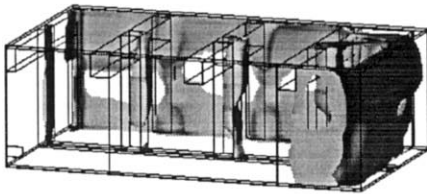
(6) The dose rate profiles do not drop much in



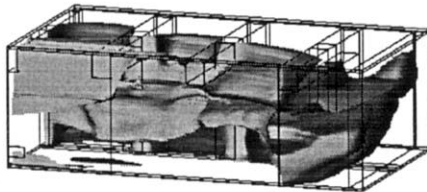
(e) Isosurface 0.1 Micro-Sv/hr



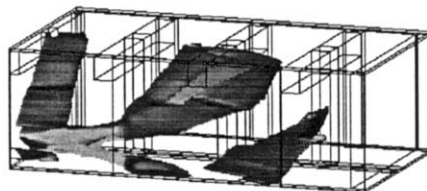
(b) Isosurface 1.0 Micro-Sv/hr



(c) Isosurface 10 Micro-Sv/hr



(d) Isosurface 100 Micro-Sv/hr



(e) Isosurface 1000 Micro-Sv/hr

Fig. 9. Isosurfaces of dose rate inside the underground rectangular part of the Tritium building.

values after 1-month from shutdown. The reduction at this time frame varies from a factor of 2 to  $\sim 1.1$  compared to 1-week after shutdown dose rates.

#### 4.3. Accessibility to the Building (Cases B and C)

Zone classification during operation and after shutdown inside ITER building were identified based on the results shown in Figs. 7, 10 and 11, and Table 1. It is shown that this desired zone classification can not be met in Case A inside the NBI hall, the access area below the cryostat, and inside the Divertor hall, even after 1-month from shutdown. Fig. 14 shows an example of this classification for Case B and Case C at 1-week after shutdown. Table 2 summarizes the classification for the three cases. From these results, the following can be stated for Cases B and C:

(1) Accessibility to the halls above ground is always permissible during operation and at any time after shutdown.

(2) During operation, the pit galleries for the divertor hall and the equatorial hall are accessible at the closed port side (Case B). The Power Termination and the Tritium building Underground Far halls are also accessible at both sides of ITER building. At the NBI port side (Case C), limited accessibility (Zone C, see Table 2) is allowed only inside the pit gallery for the divertor hall.

(3) At shutdown, the NBI hall, the Divertor hall and rooms below the cryostat are inaccessible in both Cases B and C. At the closed port side (Case B), the Lower HTS vault and the Lower CTB hall are designated as Zone C (limited access) while all other rooms have unlimited access. At the NBI open port side (Case C), the Lower HTS vault, the Lower CTB hall, and the Upper CTB hall are designated as Zone C, while all other rooms are accessible.

(4) At 1-day after shutdown, the rooms below the cryostat are inaccessible on both sides of the building. At the closed port side, the equatorial hall and the divertor hall are designated as Zone C while unlimited access is allowed inside all other rooms. At the NBI open port side, the NBI hall is inaccessible while the divertor hall has limited

Table 2  
Radiation zone classification in each room/hall of ITER building during operation and at various times after shutdown for Case A, Case B, and Case C

Room/hall	During operation			At shutdown			After 1-day			After 1-week			After 1-month		
	A <sup>a</sup>	B <sup>b</sup>	C <sup>c</sup>	A	B	C	A	B	C	A	B	C	A	B	C
HTS Drain tank room	D	D	D	D	D	D	D	D	D	D	D	D	D	D	D
VV Pressure suppression tank room	D	D	D	D	D	D	D	D	D	D	D	D	D	D	D
Lower HTS vault	D	D	D	C	C	C	C	B1	B1	A	A	A	A	A	A
Lower cold termination box hall	D	D	D	D	C	C	C	B1	B1	A	A	A	A	A	A
Divertor hall	D	D	D	D	D	D	D	C	C	D	D	D	D	D	D
Equatorial NBI hall	D	D	D	D	D	D	D	C	C	D	D	D	D	D	D
Upper HTS vault	D	D	D	D	B1	B2	D	A	B1	A	A	B1	A	A	A
Pit gallery for lower cold termination box gallery	D	D	D	C	B1	B1	B2	A	A	A	A	A	A	A	A
Pit gallery for divertor	D	A	C	C	A	A	A	B1	A	A	A	A	A	A	A
Pit gallery for equatorial hall	D	A	D	D	A	A	D	A	A	A	A	B1	A	A	A
Tritium building underground near hall	D	C	D	D	A	B1	C	A	A	B1	A	A	B1	A	A
Tritium building underground far hall	D	A	B2	A	A	A	A	A	A	A	A	A	A	A	A
Tokamak hall	A	A	A	A	A	A	A	A	A	A	A	A	A	A	A
Tritium building upper ground near hall	A	A	A	A	A	A	A	A	A	A	A	A	A	A	A
Tritium building upper ground far hall	A	A	A	A	A	A	A	A	A	A	A	A	A	A	A

<sup>a</sup> Case A.

<sup>b</sup> Case B.

<sup>c</sup> Case C.

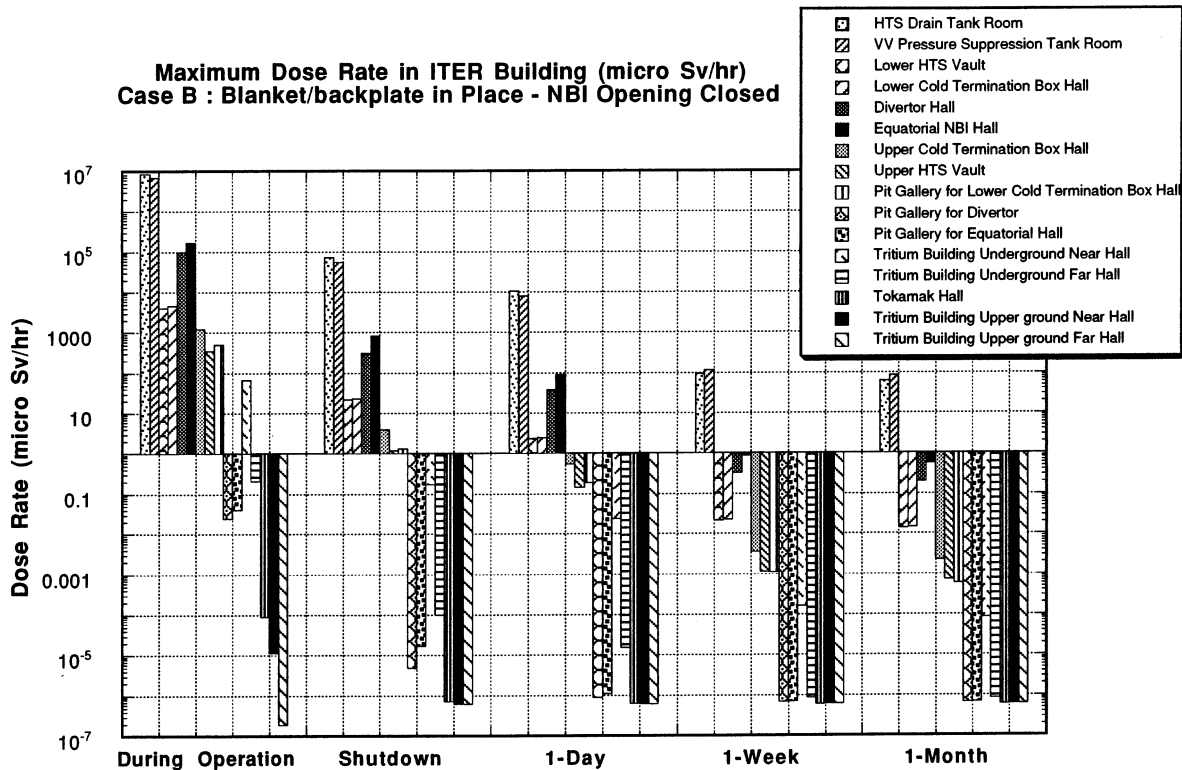


Fig. 10. Maximum dose rate inside each hall/room and gallery of ITER building during operation and at various times after shutdown, Case B.

access (Zone C). All other rooms have unlimited access.

(5) After 1-week from shutdown, the rooms below the cryostat are designated as Zone C at both sides of the building. Unlimited access inside all other rooms of the entire building is envisioned, except inside the NBI hall at the open port side (Case C).

(6) At 1-month after shutdown, the zone classification is the same as for 1-day following shutdown. This is due to decay gamma-rays not decreasing much within this time frame, although the maximum dose rates are closer to the lower bounds of the zone classification shown in Table 2.

From the above, it can be noted that the NBI cell (of Case C) cannot be accessed, even after 1-month from shutdown (maximum dose rates:  $\sim 4 \times 10^6$   $\mu\text{Sv h}^{-1}$  after 1-day,  $\sim 6.2 \times 10^5$   $\mu\text{Sv h}^{-1}$  after 1-week, and  $\sim 2.2 \times 10^5$   $\mu\text{Sv h}^{-1}$  after

1-month). Hands-on maintenance criterion (dose class B2 of  $3\text{--}10$   $\mu\text{Sv h}^{-1}$ ) on the NBI structure and immediate surroundings are not met. Full or assisted remote handling is needed in the NBI cell. On the other hand, at the side of the closed equatorial ports (Case B), the hands-on maintenance criterion is met inside every room/hall (except inside rooms below the cryostat) at 1-week from shutdown.

## 5. Summary and conclusions:

Dose rate profiles inside each hall/room and gallery of ITER building during operation and at various times after shutdown have been assessed based on extensive 2-D and 3-D discrete ordinates transport and activation calculations. Three cases are considered, namely, Case A (the FW/blanket/backplate is removed in front of a large 2.53 m

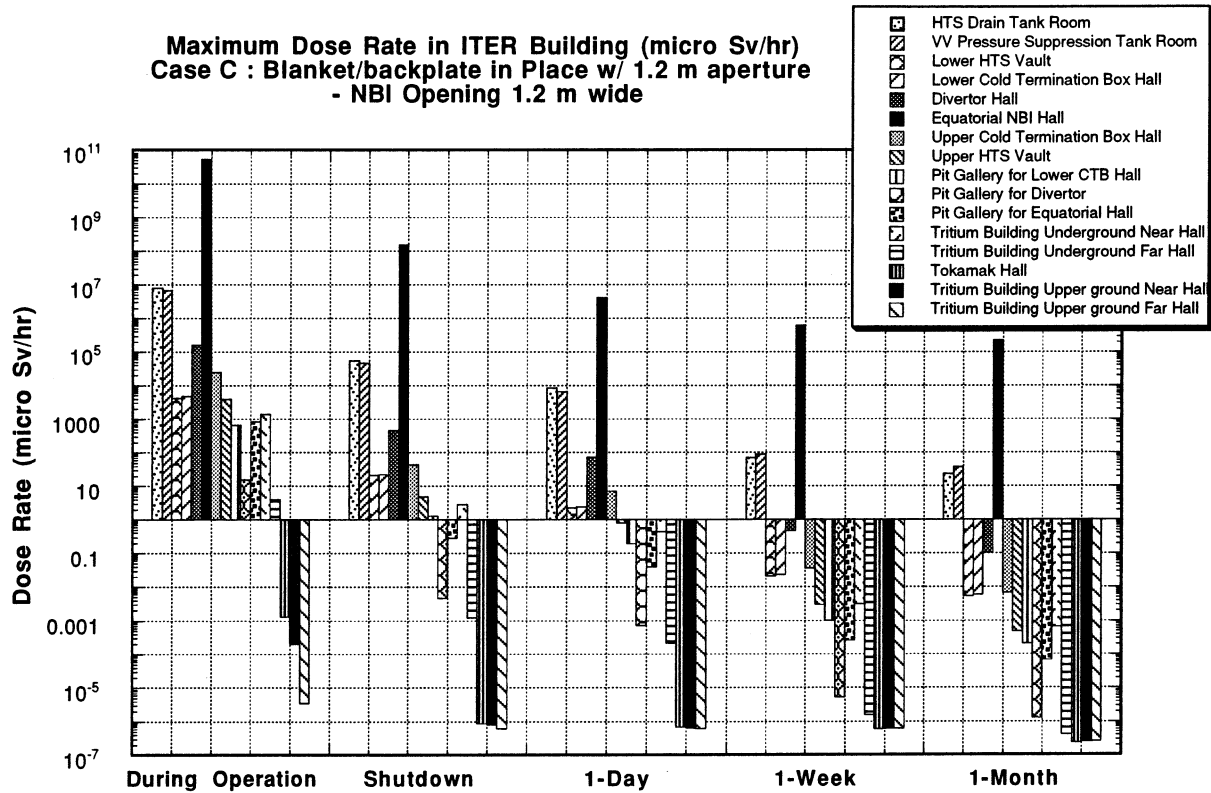


Fig. 11. Maximum dose rate inside each hall/room and gallery of ITER building during operation and at various times after shutdown, Case C.

wide horizontal opening at the NBI port), Case B (represents a plugged horizontal port away from the open ports of the NBI openings, the FW/blanket/backplate are in place), and Case C [the FW/blanket/backplate is partially removed in front of a narrow (1.2 m wide) horizontal opening at the NBI port and the NBI tube, structure and magnetic shield are considered]. Case C is a more realistic representation of the configuration at the NBI opening.

By examining the hands-on maintenance criterion set fourth for ITER (dose  $\sim 3\text{--}10 \mu\text{Sv h}^{-1}$ ), it was shown that this criterion is satisfied at all times after shutdown in the halls above ground, even during operation. For the conservative Case A, the dose rates are excessively high inside the equatorial NBI hall and inside the access halls above and below (divertor hall). These areas are inaccessible, even after 1-month following shut-

down. In Case C, all the halls/vaults and galleries are accessible 1-week after shutdown, except inside the NBI hall whose dose rate ( $6.2 \times 10^5 \mu\text{Sv h}^{-1}$ ) exceeds the required zone classification B2 ( $3\text{--}10 \mu\text{Sv h}^{-1}$ ). All halls/vaults and galleries are accessible 1-week after shutdown in Case B which represents the building side away from the NBI ports. However, in all the cases considered, the accessibility criterion inside the rooms beneath the cryostat (HTS area) is not met at all times after shutdown due to the rather thin bottom bioshield (50 cm) which may necessitate some design changes.

For the results of Case B to be valid, total isolation (shielding) between the NBI cell and those areas in the vicinity of the closed equatorial ports on the other side is needed. There is very steep gradient in the dose rate inside the equatorial hall as one moves from the vicinity of an open



Fig. 12

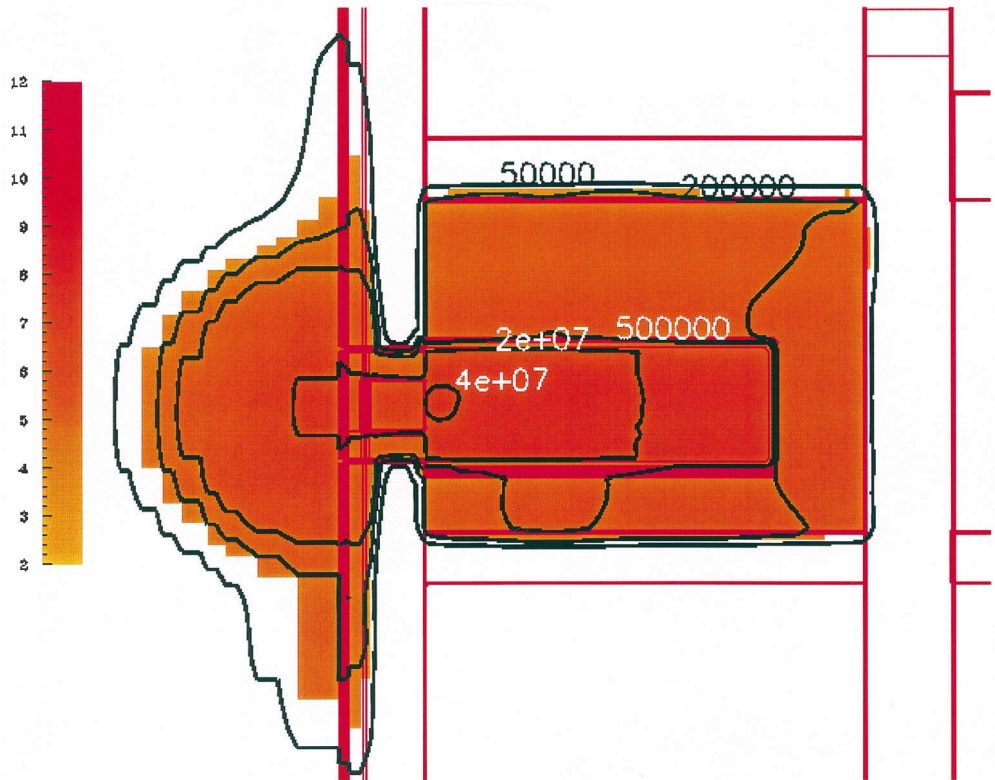


Fig. 13

Fig. 12. Color mapping of the dose rate profiles in ITER building at shutdown, Case C.  
 Fig. 13. Color mapping of the dose rate profiles in equatorial NBI Hall 1-week after shutdown, Case C.

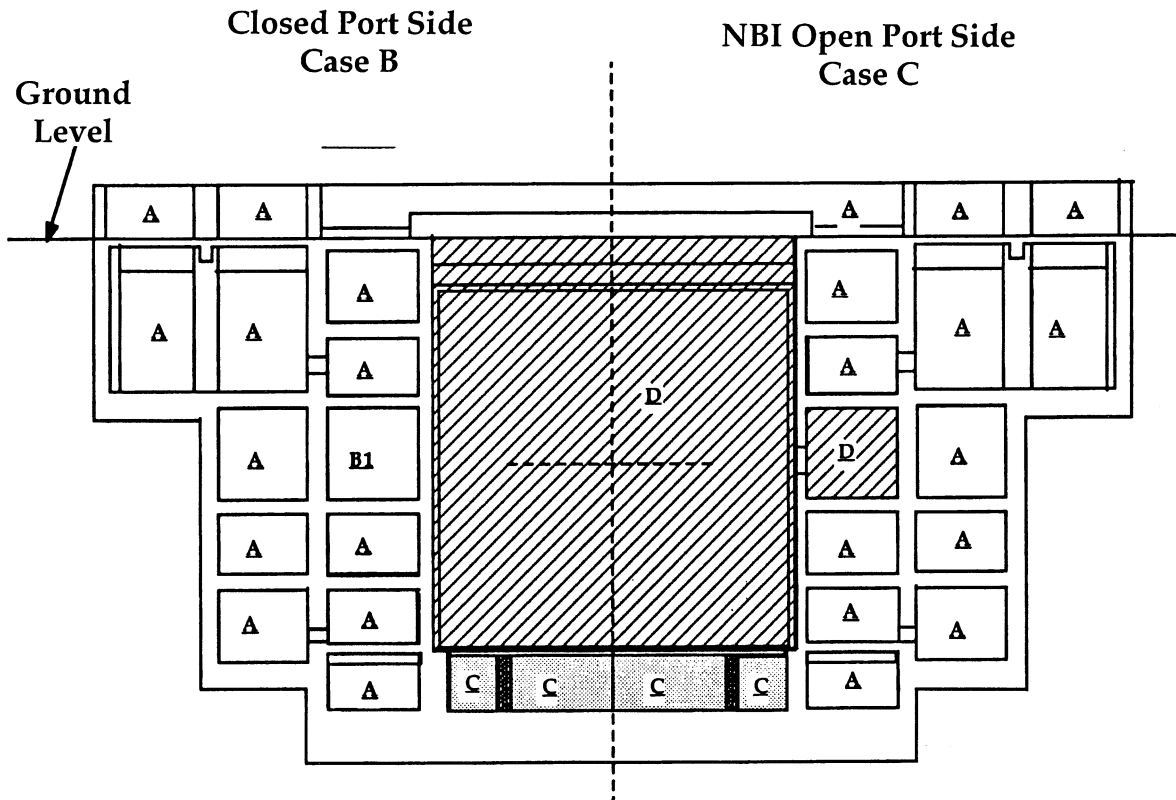


Fig. 14. Estimated zone classification for accessibility inside ITER building 1-week after shutdown, Case C.

NBI port to a closed port on the other side. At shutdown, the maximum dose rate in the NBI cells is  $\sim 1.5 \times 10^8 \mu\text{Sv h}^{-1}$  (Case C) while away from the NBI open port (Case B), the corresponding value is  $\sim 800 \mu\text{Sv h}^{-1}$  (approximately 6 orders of magnitude difference). In order to fulfill the additional shielding requirements for the hot cells located in the NBI hall to allow accessibility to the neighboring cells, accurate assessment of the dose rate variation in the toroidal (azimuthal) direction is needed through a comprehensive  $R-\theta-Z$  calculations, at least for the equatorial NBI level. On the other hand, if accessibility to the NBI cells is required, say 1-week after shut down, one should reduce the maximum dose inside the NBI structure ( $5 \times 10^7 \mu\text{Sv h}^{-1}$ ) by at least 7 orders of magnitude to reach a level of  $\sim 5 \mu\text{Sv h}^{-1}$  (zone class B2). This can be realized if the outer surface of the NBI structure is covered by a shielding material that is thick enough to attenuate the dose rate to the level

required for the hands-on maintenance. This was recently examined in a study that focused only on the NBI hall [13]. In addition to the 20 cm thick magnetic shield assumed in the present study,  $\sim 50\text{--}60$  cm of multi-layers of strong neutrons and gamma-rays absorber is needed. This additional shield could be optimized such that the inner layers are made of SS316 while the outer layers are made of B4C/Pb. The feasibility of adding this extra shield to the NBI structure should be investigated to ensure that the functionality of the NBI is not impaired.

The present work focuses only on the activation of the concrete building of ITER due to streaming of neutrons and gamma rays during operation without accounting for activation of equipment placed inside the building (e.g. HTS equipment and cooling pipes in the upper and lower vaults, V.V. Suppression Tank, etc.). This additional contribution to the overall dose rates should be assessed

(including contribution from activated and tritiated water, corrosion products, humidity in air, etc.) prior to licensing ITER for construction. In addition, the dose from performing several maintenance scenarios by transporting activated components from the inside of the cryostat to servicing halls and galleries in the building should be further examined. Most of the equipment specifications and planned scenarios for maintenance will be well defined by the end of the EDA phase and therefore, these additional assessments are most suited to be undertaken during the transition period prior to ITER construction.

### Acknowledgements

The authors would like to thank R. Santoro and D. Dilling for their support, information and specifications provided with regard to ITER building. Thanks also to J. Eggleston for assistance with the compilation and testing of DORT/TORT system. This report is an account of work assigned to the US Home Team under Task Agreement No.S 62 TD 12 ID No: D325 within the Agreement among the European Atomic Energy Community, the Government of Japan, the Government of the Russian Federation, and the Government of the United States of America on Cooperation in the Engineering Design Activities for the International Thermonuclear Experimental Reactor (ITER EDA Agreement) under the auspices of the International Atomic Agency (IAEA).

### References

- [1] M.Z. Youssef, et al., Report on ITER Task S62 TD12, ID

- no: D325: Three Dimensional Calculations of Building Dose Rate Profiles, ITER Document, UCLA-FNT-100, UCLA-ENG-98-190, University of California, Los Angeles, April 1998.
- [2] Technical Basis for the ITER Detail Design Report, Cost, Review and Safety Analysis, ITER Document, International Thermonuclear Experimental Reactor, November 1996.
- [3] C.E. Ahlfeld, D.A. Dilling, Z. Ishimoto, S. Stoner, E. Tanaka, ITER Tokamak buildings and equipment layout, Fusion Technol. 30 (1996) 611-617.
- [4] W. A. Rhoades, et al., DORT-TORT Two and Three-Dimensional Discrete Ordinates Transport Version 2.8.14, CCC-543, Radiation Shielding Information Center (RSIC), June 1994.
- [5] J.E. Eggleston, M.A. Abdou, M.Z. Youssef, The use of MCNP for neutronics calculations within large buildings of fusion facilities, Fusion Eng. Des. 42 (1998) 281–288.
- [6] K. Maki, et al., Nuclear Group Constant Set Fusion-J3 for Fusion Reactor Nuclear calculations based on JENDL-3, JAERI-M 91-72, Japan Atomic Energy Research Institute, 1991.
- [7] A.B. Pashchenko, Completion of FENDL-1 and Start of FENDL-2, INDC(NDS)-352, IAEA Nuclear Data Section, International Atomic Energy Agency, March 1996.
- [8] S. Ganesan, D.W. Muir, FENDL Multigroup Libraries, IAEA-NDS-129, International Atomic Energy Agency, July 1992.
- [9] R.E. MacFarlane, TRANSX2: A Code for Interfacing MATXS Cross-Section Libraries to Nuclear Transport Codes, LA-12312-MS, Los Alamos National Laboratory, July 1992.
- [10] P. Grande, M.C. O'Riordaw, Data for Protection Against Ionizing Radiation from External Sources, ICRP-21, International Commission on Radiological Protection, Pergamon, Oxford, April 1971.
- [11] D.L. Henderson, O. Yasar, DKR-ICF: A Radioactivity and Dose Rate Calculation Code Package, UWFD-714, vol. 1, University of Wisconsin, April 1987.
- [12] D. Dilling, Radiation Zones and Personnel Access in the Tokamak Building, S 62 MD 1 9604-10 F 1, ITER Memorandum, ITER San Diego working site, April 1996.
- [13] T. Inoue, K. Shibata, Y. Ohara, Y. Okumura, Neutronics of ITER NBI 16.7 MW System, ITER NBI review meeting, Le Chateau de Cadarache, July 1996.